Dynamic identification of prestressed reinforced concrete railway bridges through Automated Operational Modal Analysis: an example on two case studies

Available online at www.sciencedirect.com

ScienceDirect

Procedia Structural Integrity 78 (2026) 317–324

Structural Integrity Procedia

www.elsevier.com/locate/procedia

XX ANIDIS Conference

Dynamic identification of prestressed reinforced concrete railway bridges through Automated Operational Modal Analysis: an example on two case studies

Eleonora Massarelli[a], Marco Civera[a]*, Giulio Ventura[a], Bernardino Chiaia[a]

[a] *Department of Structural, Geotechnical and Building Engineering (DISEG), Politecnico di Torino, Corso Duca degli Abruzzi, 24, 10129 Turin, Italy*

Abstract

Structural Health Monitoring (SHM) of strategic transportation infrastructures is becoming increasingly important due to ageing and degradation, particularly in the case of railway bridges and viaducts that support high-speed train operations. This study presents the experimental dynamic identification of two prestressed reinforced concrete (PRC) railway bridges, representative of two common short-to-medium span typologies. The accelerometric data were acquired under operational conditions, hence, recording both ambient vibrations and train passage-induced high-amplitude vibrations. After discarding these latter disturbances, Ambient Vibration Tests (AVT) were performed through a recently-introduced Automated Operational Modal Analysis (AOMA) algorithm to identify the modal parameters (natural frequencies, damping ratios, and mode shapes), which serve as damage-sensitive features. The results of this dynamic identification are then benchmarked against those obtained with state-of-the-art commercial software (ARTeMIS), confirming the accuracy and reliability of the proposed approach.

Keywords: automated operational modal analysis; dynamic identification; structural health monitoring; high-speed railway bridge; vibration-based monitoring

* Corresponding author. Tel.: +39 0110904911
E-mail address: marco.civera@polito.it

10.1016/j.prostr.2025.12.041

1. Introduction

Railways are a critical component of civil transportation infrastructures. Among their elements, railway bridges are particularly vulnerable due to exposure to various degradation mechanisms that can compromise structural integrity and, consequently, the safety of passengers and freight. For instance, (D'Angelo et al., 2025) reports nine railway bridge failures in Italy only in the 2000-2023 period. That corresponds to an annual yearly failure rate of $2 \cdot 10^{-5}$, which is lower than for road bridges. However, these statistics also reflect the major attention dedicated to the monitoring and maintenance of railway bridges, since their serviceability limits are much stricter (European Commission, 2016). In fact, given that different components of a railway infrastructure are connected by the superstructure, i.e. the ballast and the rails, even minor structural changes, which do not pose direct structural risk on their own, might cause derailment and potentially fatal accidents.

The risk associated with railway bridges is thus primarily driven by the higher severity of potential consequences and is increasingly influenced by the growing vulnerability of the existing bridge portfolio. In Europe, it was estimated that about 35% of over 300,000 railway bridges exceed 100 years of operational life (Paulsson et al., 2010). In particular, in Italy, the majority of railway viaducts constructed between the 1950s and 1970s consist of prestressed reinforced concrete bridges (PRC) (Biondini et al., 2021). Special attention should be given to these ageing infrastructures, which are nowadays facing the effects of material degradation, corrosion of reinforcement, prestress losses, increased live loads (due to ever-increasing rail traffic), and also possible construction errors (e.g., grouting defects of prestressing sheaths and tendons ducts).

These processes can all potentially compromise safety before visible damage can be visually detected in surveys. Thus, periodic inspections, although being a fundamental tool, are not totally effective and often cannot detect early-stage damage. Vibration-based Structural Health Monitoring (SHM) addresses this problem by using data acquired through sensors to extract damage-sensitive features (DSFs), such as natural frequencies, damping ratios, and mode shapes. Possible changes in these modal parameters over time could be indicative of both global or local damages.

This contribution presents the results of an automated output-only dynamic identification approach on two PRC railway bridges under operational conditions, representative of the behaviour of two different, common short- to medium-span railway bridge typologies. The data acquired through high-sensitivity accelerometers placed on some spans of the two case studies were processed using the proposed Automated Operational Modal Analysis (AOMA) algorithm developed in MATLAB environment, based on the Stochastic Subspace Identification (SSI) algorithm (Van Overschee & De Moor, 1996). Modal parameters of the structures' decks were successfully extracted, providing repeatable and comparable results between nominally identical spans. To assess the accuracy and reliability of the proposed methodology, the results were compared with those obtained with the commercial software ARTeMIS, validating the effectiveness of the proposed automated dynamic identification approach.

The remainder of this paper is organised as follows. Section 2 describes the two case studies, the dynamic monitoring system and the acquired data. In Section 3, the AOMA procedure is briefly described. The results obtained considering the environmental excitation of the structure are then reported in Section 4, followed by the comparison with the outcomes from the commercial software ARTeMIS. The conclusions follow in Section 5.

2. Experimental test campaign

2.1. Description of the case studies

As mentioned, the two railway viaducts examined in this study are characterised by a PRC deck but (slightly) differ in their structural configurations. One (case study A) features a girder deck system; the other (case study B) a closed-section box girder deck. PRC beams and deck elements are widely employed in railway bridges due to their performance under dynamic loading conditions, such as those associated with high-speed train passages. Indeed, as mentioned, very low deflections and vibration amplitudes are needed for safety and serviceability reasons; hence, such structures are characterised by high stiffness and low vibrations under operating conditions.

Case study A consists of 46 simply supported spans, all 20 m long, for a total length of 920 m. The deck consists of eight PRC girders with I cross-sections, connected by a 20 cm-thick upper slab, and four transversal beams. The total width of the deck is approximately 12.40 m, being the main girders spaced 1.20 m and considering the two lateral cantilevers, thus allowing the support of two train tracks (see Figure 1 (a)). The viaduct is supported by RC piers having pseudo-rectangular cross-sections, with heights ranging from 2.5 m to 5 m, and whose foundation plinths lie on deep foundations (piles).

The other examined structure, case study B, is composed of 7 simply supported spans, each one 35.10 m long, for a total longitudinal length of the viaduct of 245.70 m. The deck width is approximately 9.80 m, even in this case, accommodating two train tracks. The deck is characterised by a PRC lightened box section slab with post-tensioned unbonded tendons, where the minimum height of the cross-section is 2.44 m (see Figure 1 (b) and Figure 2 (c)). The reinforced concrete piers, of either 4.00 m or 5.30 m height, present a tapered rectangular cross-section. Each pier is supported by a slab foundation on piles, as well as the abutments, which are of the reinforced concrete box-type.

(a) (b)

Figure 1: Typical spans for the two case studies: the railway viaduct with PRC girder beams deck, case study A (a) and the one with box girder PRC deck, case study B (b).

2.2. Hardware system and sensor setup

The experimental campaign aimed to identify the modal parameters of the two viaducts under operational conditions. Owing to their modular design, only a subset of spans was instrumented—three spans in case study A and two in case study B. In each monitored span, four uniaxial accelerometers were installed to measure vertical acceleration, as shown in Figure 2(a-c). This configuration allowed the identification of both vertical flexural and torsional modes.

Regarding the hardware instrumentation, in prestressed RC beams, internal compressive forces are applied before the beam is loaded; this pre-compression limits deflection and delays or prevents cracking in the concrete under service loads. As uncracked concrete has a higher flexural stiffness (modulus of elasticity × gross moment of inertia), the beam is supposed to behave more rigidly, thus with lower amplitude vibrations. To account for this, accelerometers with higher amplitude sensitivity and low background noise were chosen. Specifically, PCB piezoelectric accelerometers model 393B12 were used, with a sensitivity of 10 V/g and a noise of 0.32 $\mu g/\sqrt{Hz}$ on the 10 Hz band, connected to a 24-bit acquisition system.

The accelerometric signals included both ambient vibrations and train-induced responses. To isolate ambient vibrations, recordings containing train passages were segmented, and only continuous portions longer than four minutes were retained; this lower bound aligns with the ranges recommended in (Rainieri & Fabbrocino, 2014) for reliable damping estimation—typically 1000 to 2000 times the natural period of the first mode.

This resulted in 80 usable recordings for case study A (with 28, 29, and 23 signals for the three instrumented spans respectively) and 74 for case study B (respectively 31 and 43 for spans #1 and #2). The latter one is positioned in a railway line where traffic is higher, resulting in a greater number of train passages and shorter ambient vibrations, although still of appropriate durations. All data were acquired at a sampling rate of 100 Hz, such that the Nyquist limit $f_s/2 = 50$ Hz was well above the highest frequencies of interest (approximately 16 Hz for case study A and 15 Hz for case study B, as will be shown in the following Sections).

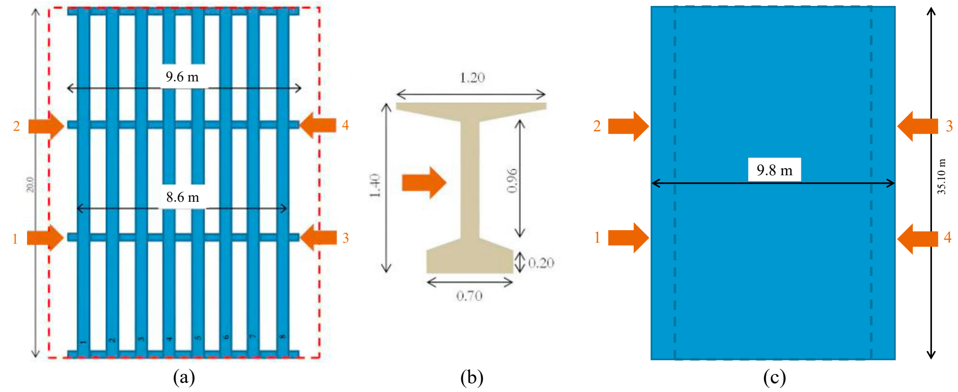

Figure 2: Scheme of the typical span for case study A (a) and position of the accelerometers on the main beams near the cross beams (b). Scheme for the typical span of case study B and sensors positions (c). In all figures, the numbers in red (1 to 4) indicate the position of the different output channels (all oriented along the vertical).

3. Automated Operational Modal Analysis for SHM

Automated Operational Modal Analysis (AOMA) procedures are designed to extract modal parameters from structural vibration data through a sequence of automated steps, starting after system identification over increasing model orders. These steps include a series of pole filtering passes and then the estimation and validation of cluster-level modal parameters (Magalhães et al., 2009; Ubertini et al., 2013).

In this study, the dynamic identification of the bridge decks was performed using the Stochastic Subspace Identification (SSI) algorithm (Van Overschee & De Moor, 1996). This technique produces a set of system poles. As hinted, when run multiple times on the same signals with increasing model order, the results are typically visualised in a stabilisation diagram, which displays natural frequencies, damping ratios, and mode shapes relative to the assumed system order. However, the raw output includes both physical and spurious (mathematical) poles, making a filtering process essential.

Several authors have proposed procedures to address the automatic interpretation of the stabilisation diagram and the subsequent extraction of the physically meaningful vibration modes (Rainieri & Fabbrocino, 2015; Reynders et al., 2012). All consists of defining a set of physically-principled ("hard") or data-driven ("soft") validation criteria to distinguish possibly physical poles from certainly spurious ones. The steps used here to enable this procedure, as adopted in the presented methodology, are briefly outlined below:

- hard validation criteria (HVC), consisting of the elimination of poles with non-physical damping ratios, hence negative or excessively high (here, > 20%), and those with eigenvectors not being complex conjugate pairs;
- soft validation criteria (SVC), concerning the comparison between the modal parameters of the different poles and elimination of those exceeding the selected thresholds, following the work by Mugnaini et al. (2022);
- application of the DBSCAN algorithm (Ester et al., 1996) to group the poles with similar modal features and discard any outliers, similarly to what was proposed by Civera et al. (2023).

In particular, the specific algorithm applied here was also recently reported in Massarelli et al. (2025) .

Each resulting cluster is then associated with a probable physical mode. Modal parameters for each cluster — namely, the natural frequency f_n and the damping ratio ξ_n — are estimated as the average values of the poles within the cluster (Reynders et al., 2012).

4. Results

4.1. AOMA algorithm results

The SSI algorithm needs the definition of two fundamental user-defined parameters, the range of model order, here set from n_{min} = 20 to n_{max} = 130, and the number of block rows of the Hankel matrix, here defined as $i = f_s/2$ (Van Overschee & De Moor, 1996). The stabilisation parameters for the stabilisation diagram were set equal to: $df < 0.005$;

$0 < d\xi < 0.1$; and MAC < 0.95, following Civera et al. (2023). Overall, these settings were seen to give consistent results for all datasets of the two case studies; hence, they were kept fixed for both to guarantee better comparability.

The final, cleaned stabilisation diagrams are reported in Figure 3, after the clustering phase (the colours reflect the different clusters). The specific signals are taken from example datasets of one of the instrumented spans for each case study. In both cases, the frequency range of interest was limited up to 20 Hz, where clear peaks can be observed in the singular values plotted alongside the identified poles.

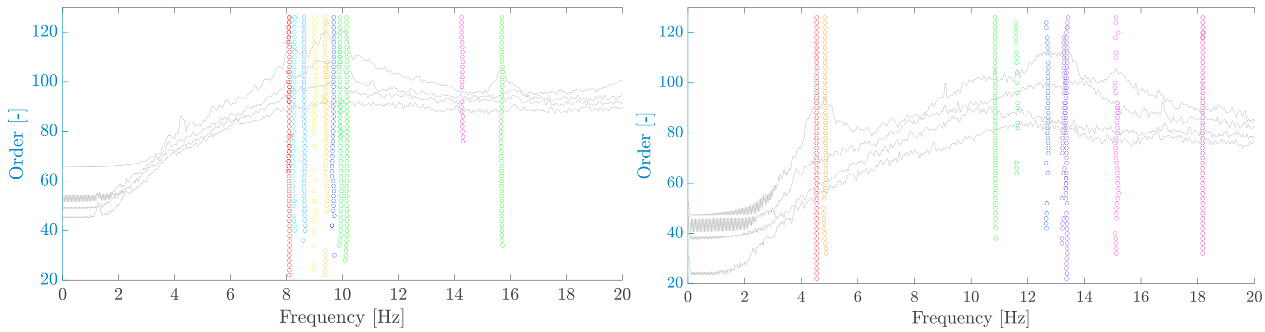

(a) (b)

Figure 3: Example of stabilisation diagram with identified clusters and singular values superimposed for case study A (a) and case study B (b).

Figure 4 presents, by means of example, the histograms of the identified natural frequencies across all ambient vibration recordings for one span of both case studies. The dominant frequencies, corresponding to physically meaningful modes, were determined by comparing all results from individual segments. Similar results were found for the other spans as well.

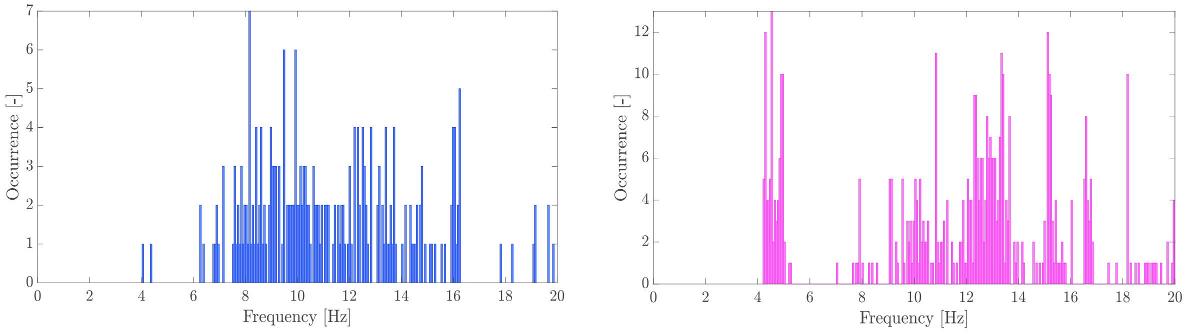

(a) (b)

Figure 4: Example of histograms of the occurrence of identified natural frequencies of probable physical modes for one span of case study A (a) and case study B (b).

The full set of natural frequencies obtained by application of the AOMA technique to the presented case studies is summarised in Table 1, for each span of the two viaducts. Finally, Figure 5 illustrates the experimental mode shapes for the most relevant modes. In case study A, the first torsional mode was detected twice and labelled as Mode 2a and 2b. A similar pattern was found in case study B, where two closely spaced first flexural modes (Mode 1a and 1b) were observed, along with two identifications of the first torsional mode (Mode 2a and 2b).

These duplicate identifications may arise from the use of vertical-only sensors. In such configurations, the effects of lateral modes may remain detectable in the signals' frequency, even if the mode shapes are not measured along their main direction of vibration, thus leading to an apparent doubling of the closely spaced vertical modes.

Additionally, a further mode was identified in case study A (Mode 3), likely associated with deck behaviour not fully captured by the current sensor layout (Figure 5 (d)). The Authors' educated guess is that it could be some plate-like mode of the deck. A higher-order torsional mode (Mode 3) was instead found in case study B (Figure 5 (i)).

Table 1: Summary of the modal parameters identified by the AOMA MATLAB code for the relevant modes in the instrumented spans in case study A (left) and B (right), with average and standard deviation values (St.Dev).

		Case study A				Case study B				
		Mode 1	Mode 2a	Mode 2b	Mode 3	Mode 1a	Mode 1b	Mode 2a	Mode 2b	Mode 3
Span 1	f [Hz]	8.148	9.205	10.084	15.873	4.300	4.847	12.821	13.352	15.169
	ξ [-]	0.016	0.019	0.021	0.010	0.027	0.045	0.015	0.012	0.021
Span 2	f [Hz]	8.117	9.181	10.112	16.020	4.301	4.799	12.829	13.349	15.104
	ξ [-]	0.019	0.017	0.014	0.011	0.026	0.036	0.012	0.014	0.019
Span 3	f [Hz]	8.126	9.142	10.123	15.907	n.a.	n.a.	n.a.	n.a.	n.a.
	ξ [-]	0.026	0.016	0.020	0.012	n.a.	n.a.	n.a.	n.a.	n.a.
Average	$\boldsymbol{f}$ **[Hz]**	**8.130**	**9.176**	**10.106**	**15.933**	**4.300**	**4.823**	**12.825**	**13.351**	**15.136**
	$\boldsymbol{\xi}$ **[-]**	**0.020**	**0.017**	**0.018**	**0.010**	**0.027**	**0.041**	**0.014**	**0.013**	**0.020**
St.Dev.	$\boldsymbol{f}$ **[Hz]**	**0.016**	**0.032**	**0.020**	**0.077**	**0.0005**	**0.034**	**0.006**	**0.002**	**0.046**
	$\boldsymbol{\xi}$ **[-]**	**0.005**	**0.002**	**0.004**	**0.001**	**0.001**	**0.007**	**0.002**	**0.002**	**0.001**

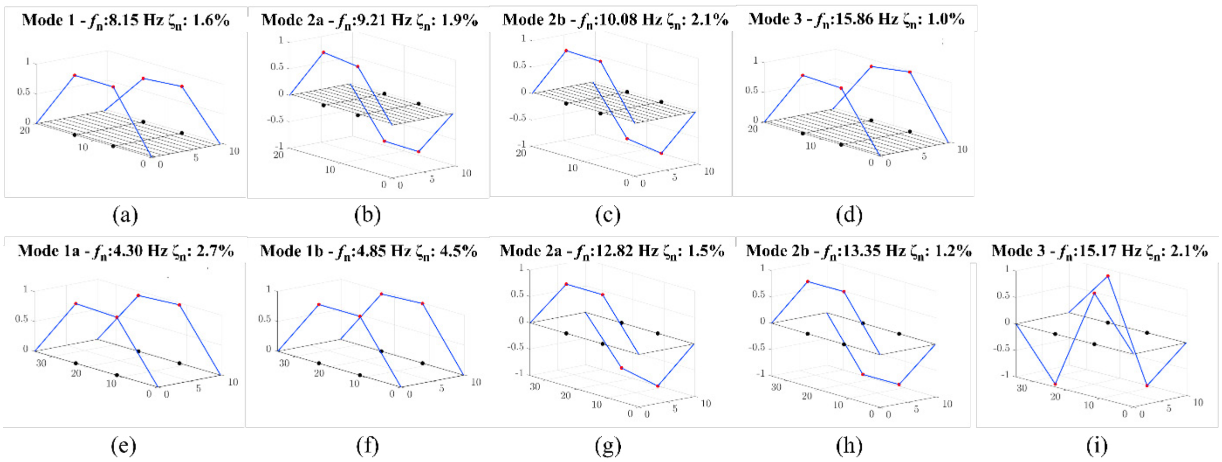

Figure 5: Identified mode shapes for one span for each structure with an indication of the measurement points in red, the top part refers to case study A [mode 1 (a), modes 2a (b), and 2b (c), and possibly a plate-like mode 3 (d)]; and for case study B in the bottom part [modes 1a (e) and 1b (f), modes 2a (g), and 2b (h), and mode 3 (i) of higher order].

4.2. ARTeMIS benchmark results

To validate the results, the same datasets were processed using ARTeMIS using the Stochastic Subspace Identification variant with Unweighted Principal Component (SSI-UPC) algorithm†. The signals relative to ambient vibrations used are those from the pre-processing phase described in Section 2.2, hence ensuring comparable results. Identical model order ranges and stabilisation parameters were used for consistency.

The same double identifications were again observed, confirming that the phenomenon is almost certainly physically meaningful and not due to some technical issue in the identification algorithm developed in MATLAB.

The results are reported in Table 2. This can be compared to the ones from the previous Table 1. In general, ARTeMIS produced slightly higher damping ratios compared to the Authors' estimates, reflecting known

† https://www.svibs.com/resources/ARTeMIS_Modal_Help_v3/SSI_ssi.htm

uncertainties in damping evaluation (Reynders et al., 2008). On the other hand, natural frequencies show great consistency, with the averaged results never deviating more than 1.8% (which is in line with statistical fluctuations, generally assumed as ±2%).

Unfortunately, due to the page limit, it is not possible to report here completely on the Modal Assurance Criterion between mode shapes of different spans, or between ARTeMIS and MATLAB. Summarising, the results for case study A show how the mode shapes extracted for the different spans are superimposable, as a testament to the quality of the data acquired, even though with slightly different frequencies, especially for the first torsional modes reported as 'Mode 2a' and 'Mode 2b' in both cases, as denoted by the higher standard deviation values. Similar considerations can be done for case study B. Nevertheless, the results from the commercial software ARTeMIS, considering the first three modes, indicate a good correlation with the outcomes of the proposed MATLAB code in terms of natural frequencies and mode shapes (for all spans and both case studies).

Table 2: Summary of the modal parameters identified with ARTeMIS for the relevant modes in the instrumented spans of case study A (left) and B (right) with ARTeMIS' SSI-UPC method, with computation of the average and standard deviation values (St.Dev).

		Case study A				Case study B				
		Mode 1	Mode 2a	Mode 2b	Mode 3	Mode 1a	Mode 1b	Mode 2a	Mode 2b	Mode 3
Span 1	f [Hz]	8.461	9.631	10.030	15.777	4.321	4.822	12.854	13.312	15.270
	ξ [-]	0.072	0.048	0.063	0.015	0.043	0.044	0.029	0.021	0.031
Span 2	f [Hz]	8.171	9.168	10.197	16.092	4.275	4.756	13.247	13.501	14.971
	ξ [-]	0.054	0.046	0.044	0.017	0.042	0.069	0.036	0.046	0.029
Span 3	f [Hz]	8.125	9.231	10.320	16.217	n.a.	n.a.	n.a.	n.a.	n.a.
	ξ [-]	0.049	0.058	0.045	0.014	n.a.	n.a.	n.a.	n.a.	n.a.
Average	$\boldsymbol{f}$ **[Hz]**	**8.252**	**9.343**	**10.182**	**16.029**	**4.298**	**4.789**	**13.050**	**13.406**	**15.121**
	$\boldsymbol{\xi}$ **[-]**	**0.058**	**0.051**	**0.050**	**0.015**	**0.043**	**0.056**	**0.033**	**0.034**	**0.030**
St.Dev.	$\boldsymbol{f}$ **[Hz]**	**0.182**	**0.251**	**0.145**	**0.227**	**0.032**	**0.047**	**0.277**	**0.133**	**0.211**
	$\boldsymbol{\xi}$ **[-]**	**0.013**	**0.006**	**0.011**	**0.002**	**0.0005**	**0.018**	**0.005**	**0.018**	**0.001**

5. Conclusions

This study investigated the application of a recently proposed Automated Operational Modal Analysis (AOMA) algorithm, developed in MATLAB, for Structural Health Monitoring (SHM) of railway viaducts. The methodology was tested on two prestressed reinforced concrete (PRC) bridges representative of typical short- to medium-span railway structures. High-sensitivity accelerometers were installed on selected spans, and ambient vibration data were recorded under operational conditions. The proposed AOMA approach successfully extracted modal parameters — natural frequencies, damping ratios, and mode shapes — which may serve as reliable damage-sensitive features. To assess the accuracy and robustness of the method, results were compared with those obtained using the commercial software ARTeMIS. The strong agreement in frequencies and mode shapes confirmed the effectiveness of the automated identification procedure with these two features.

The monitoring of nominally identical spans in the two case studies enabled an evaluation of variability under uniform analysis conditions. This supports the feasibility of assessing damage in one span through comparative analysis with others, either historically or synchronously in real-time.

Furthermore, while this work focused on ambient vibration segments, the free vibrations induced by passing trains also showed promise for modal parameter extraction, using alternative system identification algorithms. This aspect offers a valuable direction for future research.

Overall, in view of a broader approach to infrastructure monitoring, maintenance and management, these findings validate the feasibility of using AOMA for the continuous structural health monitoring of railway bridges.

Acknowledgements

The study presented here was carried out as part of the program of activities carried out within the MOST – Sustainable Mobility National Research Centre and received funding from the European Union Next-GenerationEU (PIANO NAZIONALE DI RIPRESA E RESILIENZA (PNRR) – MISSIONE 4 COMPONENTE 2, INVESTIMENTO 1.4 – D.D. 1033 17/06/2022).

References

Biondini, F., Manto, S., Beltrami, C., Tondolo, F., Chiara, M., Salza, B., Tizzani, M., Chiaia, B., Lencioni, A., Panseri, L., & Quaranta, L. (2021). BRIDGE|50 research project: Residual structural performance of a 50-year-old bridge. *Bridge Maintenance, Safety, Management, Life-Cycle Sustainability and Innovations - Proceedings of the 10th International Conference on Bridge Maintenance, Safety and Management, IABMAS 2020*, 3337–3344. https://doi.org/10.1201/9780429279119-453

Civera, M., Sibille, L., Zanotti Fragonara, L., & Ceravolo, R. (2023). A DBSCAN-based automated operational modal analysis algorithm for bridge monitoring. *Measurement*, *208*, 112451. https://doi.org/10.1016/j.measurement.2023.112451

D'Angelo, M., Civera, M., Giordano, P. F., Borlenghi, P., Ballio, F., Limongelli, M. P., & Chiaia, B. (2025). Bridge collapses in Italy across the 21st century: survey and statistical analysis. *Structure and Infrastructure Engineering*. https://doi.org/10.1080/15732479.2025.2483500

Ester, M., Kriegel, H.-P., Sander, J., & Xu, X. (1996). A density-based algorithm for discovering clusters in large spatial databases with noise. *Proceedings of the Second International Conference on Knowledge Discovery and Data Mining*, 226–231.

European Commission. (2016). *Directive (EU) 2016/798 Of The European Parliament And Of The Council Of 11 May 2016 On Railway Safety*.

Magalhães, F., Cunha, Á., & Caetano, E. (2009). Online automatic identification of the modal parameters of a long span arch bridge. *Mechanical Systems and Signal Processing*, *23*(2), 316–329. https://doi.org/10.1016/j.ymssp.2008.05.003

Massarelli, E., Civera, M., Ventura, G., & Chiaia, B. (2025, September 1). Preliminary results from a field application of dynamic monitoring on three spans of a railway bridge. *Proceedings of the 13th International Conference on Structural Health Monitoring of Intelligent Infrastructure (SHMII-13)*.

Mugnaini, V., Zanotti Fragonara, L., & Civera, M. (2022). A machine learning approach for automatic operational modal analysis. *Mechanical Systems and Signal Processing*, *170*, 108813. https://doi.org/10.1016/j.ymssp.2022.108813

Paulsson, B., Olofsson, J., Hedlund, H., Bell, B., Täljsten, B., & Elfgren, L. (2010). Sustainable Bridges–Results from a European Integrated Research Project. *Proceedings of the IABSE Symposium Report*, 17–24.

Rainieri, C., & Fabbrocino, G. (2014). *Operational Modal Analysis of Civil Engineering Structures*. Springer New York. https://doi.org/10.1007/978-1-4939-0767-0

Rainieri, C., & Fabbrocino, G. (2015). Development and validation of an automated operational modal analysis algorithm for vibration-based monitoring and tensile load estimation. *Mechanical Systems and Signal Processing*, *60–61*, 512–534. https://doi.org/10.1016/j.ymssp.2015.01.019

Reynders, E., Houbrechts, J., & De Roeck, G. (2012). Fully automated (operational) modal analysis. *Mechanical Systems and Signal Processing*, *29*, 228–250. https://doi.org/10.1016/j.ymssp.2012.01.007

Reynders, E., Pintelon, R., & De Roeck, G. (2008). Uncertainty bounds on modal parameters obtained from stochastic subspace identification. *Mechanical Systems and Signal Processing*, *22*(4), 948–969. https://doi.org/10.1016/j.ymssp.2007.10.009

Ubertini, F., Gentile, C., & Materazzi, A. L. (2013). Automated modal identification in operational conditions and its application to bridges. *Engineering Structures*, *46*, 264–278. https://doi.org/10.1016/j.engstruct.2012.07.031

Van Overschee, P., & De Moor, B. (1996). *Subspace Identification for Linear Systems*. Springer US. https://doi.org/10.1007/978-1-4613-0465-4